THE JOURNAL OF PHYSICAL CHEMISTRY A

Article

pubs.acs.org/JPCA

Rovibrational Dynamics of RbCs on its Lowest $^{1,3}\Sigma^+$ Potential Curves Calculated by Coupled Cluster Method with All-Electron Basis Set

Yonggang Yang,* Xiaomeng Liu, Yanting Zhao, Liantuan Xiao, and Suotang Jia

State Key Laboratory of Quantum Optics and Quantum Optics Devices, Laser Spectroscopy Laboratory, Shanxi University, Taiyuan 030006, China

Supporting Information

ABSTRACT: Relativistic ab initio potential curves of RbCs lowest $^{1,3}\Sigma^+$ states are calculated by diagonalizing the Douglas−Kroll−Hess Hamiltonian as implemented in Gaussian09 suite of programs. The ab initio calculations are performed at the CCSD(T) level with UGBS1P+ basis set, a huge all-electron basis set. The rovibrational eigenenergies and eigenfunctions on the lowest $^{1,3}\Sigma^+$ ab initio potential curves are calculated by direct diagonalization of molecular Hamiltonian in a Fourier grid discrete variable representation. The results agree well with available experimental and theoretical work and the accuracy of theoretical descriptions of RbCs are increased, which is expected to be a good reference for further investigations.

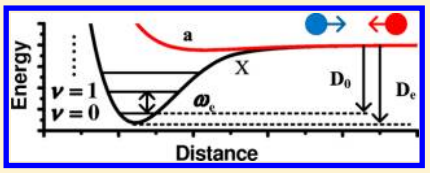

INTRODUCTION

Cold and ultracold molecules have been extensively studied both experimentally and theoretically in recent years.[1−5] Deep investigations on ultracold molecules are expected to make significant impact on various fields just as the investigations on ultracold atoms have made.[3,4] For good manipulations of ultracold molecules the preparation of their ground state ensemble is generally considered as a benchmark.[6−8] Although great progress has been achieved concerning experimental techniques to produce ultracold molecules, it is still challenging to create dense ensemble of rovibrational ground state ultracold molecules at lowest electronic state.[6−10] To meet this challenge, a detailed understanding of molecular states involving electronic, vibrational, and even rotational degrees of freedom is essential.

Among various molecules being investigated in this fast developing research area, ultracold polar molecules are of particular interest due to their large permanent dipole moments capable of efficient manipulations under an external electric field. In the past few years many experiments have produced polar alkali diatomic molecules by photoassociation[6,7,11,12] or Feshbach resonance.[13−16] For the purpose of producing dense ensemble of ultracold polar molecules RbCs has been more favored than KRb due to its stability under binary collisions at its lowest rovibrational state.[17] In 2004 DeMille group has produced the lowest singlet[18] and triplet[19] states RbCs molecules, which opens the possibility of creating a dense ensemble of ultracold ground state RbCs molecules. Soon after that, the formation of both electronic and vibrational ground state RbCs molecules has also been performed via photoassociation of laser-cooled atoms followed by a laser-stimulated state transfer process.[6] Apart from above-mentioned experiments, ultracold metastable RbCs molecules have also been observed in the short internuclear distance range after direct photoassociation in refs 20 and 21. To explore efficient ground-state transfer pathways for RbCs, two-photon high resolution spectroscopy on ultracold samples of RbCs Feshbach molecules has been performed very recently.[22]

From theoretical point of view there have been some ab initio calculations of potential energy[23−25] and dipole moment[25,26] curves of alkali dimers using different pseudo potentials to describe inner core electrons. An all-electron configuration interaction study of potentials and dipoles has also been reported recently in ref 27. Based on ab initio potentials and dipoles, it is possible to calculate various molecular properties such as polarizability and photoassociation rates. A systematic investigation of the permanent dipole moments of polar alkali dimers reaching the convergence limit of basis set has been performed[26] by the Dulieu group. With the same quantum chemistry approach they further studied the static dipole polarizabilities of these molecules and their dependence on internuclear distances and vibrational quantum numbers.[28] The calculated polarizabilities agree with available experimental data, which shows the predictability of calculations at proper quantum chemistry level. Earlier calculations on the photoassociation rates together with rates of producing ground state RbCs molecules also turn out to be good references of later experiments.[29] Very recently systematic calculations on the lifetimes of vibrational levels for excited RbCs molecules using mapped Fourier grid Hamiltonian representation method[30] have provided clues to find a good intermediate state for efficient formation of rovibrational ground state RbCs molecules. To approach the accuracy of ultracold molecule experiments, consequently providing efficient guidance to experimentalists, a fundamental prerequisite is to obtain sufficiently accurate potential energy curves. Accurate potential energy curves with which the vibrational

Special Issue: Jörn Manz Festschrift

Received: April 24, 2012
Revised: August 9, 2012
Published: August 13, 2012

energies can be obtained with errors less than 1 cm^{-1} are expected to be capable of guiding future experiments efficiently. However, this is quite challenging due to limitations of both computational methods and computers. Toward this aim this work will report the lowest $^{1,3}\Sigma^+$ states potential energy curves obtained by all-electron studies and accurate rovibrational analysis, which meets part of the challenge.

In the present work accurate rovibrational spectra of RbCs molecules at lowest $^{1,3}\Sigma^+$ states are studied on relativistic ab initio potential energy curves at the CCSD(T)/UGBS1P+ level. By combination of an all-electron basis set UGBS1P+ and the accurate quantum chemistry method CCSD(T), the calculated potential curves are expected to be convincing. Details about our numerical computations are given in the Methods section. The accuracy of the calculated potential curves are first checked by comparing with previous experimental and theoretical work then the rovibrational spectra of RbCs molecules are investigated. Finally, the conclusions of the present work are summarized.

METHODS

Quantum Chemistry Calculations. The potential curves of lowest $^{1,3}\Sigma^+$ RbCs electronic states are calculated with Gaussian09 suite of programs.[31] Different from previous calculations that resort to certain pseudopotentials to characterize inner core electrons, in this work all 92 electrons of RbCs molecule are treated explicitly by UGBS series of basis sets implemented in Gaussian09. Polarization and diffusion functions are added to all the basis functions because both the relativistic effects of inner core electrons and the interactions between valence electrons need to be well characterized. Consequently, the final basis set adopted for our ab initio potential energy calculations is UGBS1P+ containing 713 basis functions. The CCSD(T) method, coupled cluster including single and double excitations and triple excitations by perturbation, is adopted to get accurate energies. For modern quantum chemistry calculations the CCSD(T) method has been widely used for accurate energy calculations of small molecules due to its balance between speed and accuracy.

Concerning ab initio calculations involving heavy atoms such as Rb and Cs, the relativistic effect is an important issue. This has led to the generalization of various pseudopotentials to characterize relativistic effects of inner core electrons of heavy atoms as a fast numerical method. A direct consequence is that all this kind of calculations crucially rely on the quality of the adopted pseudopotentials, which leads to difficulties for comparing results obtained from different pseudopotentials. In this work the relativistic effects are treated by directly solving the Douglas−Kroll−Hess relativistic Hamiltonian[32] for all the 92 electrons of RbCs molecule as implemented in Gaussian09. An advantage of ab initio calculations with an all-electron basis set is that it is straightforward to pursue even higher accuracy step by step (for example, the increasing number of inner core electrons for post Hartree−Fock correlation treatment) and compare with other all-electron calculations. In our final ab initio calculations of RbCs lowest $^{1,3}\Sigma^+$ potential curves one more shell of inner core electrons are included for post Hartree−Fock correlation energy calculations compared to default CCSD(T) in Gaussian09. The adopted quantum chemistry level turns out to be sufficient for our main purpose of this work as will be shown in the next section. Another crucial issue for RbCs potential curves is the hyperfine spin−orbit coupling which leads to large splittings for many excited states. However, as far as our present investigations being concerned, the $^3\Sigma^+$ state has a splitting of less than 1 cm^{-1} as reported in ref 24. This can be expected because Hund's case (b) is the best approximation for Σ states. Therefore, the spin−orbit coupling is not calculated for the present lowest $^{1,3}\Sigma^+$ states. To study the dynamics or manipulation of RbCs molecules in external field, the dipole moment curves are required. In this work all the required dipole moment curves are calculated with Gaussian09 at CCSD/QZVP level of theory.

Rovibrational Analysis. Having the potential curves at hand, the rovibrational eigenfunctions can be obtained. Motions of RbCs can be described by relative motion **R** (R,θ,ϕ) between the two atoms and translation of RbCs center of mass which can be separated. The rovibrational eigenfunctions of RbCs can be written as

$$\langle \mathbf{R}|\nu Jm\rangle = \langle R,\theta,\phi|\nu Jm\rangle = \Psi_{\nu J}(R)\, Y_J^m(\theta,\phi) \tag{1}$$

where $\Psi_{\nu J}(R)$ and $Y_J^m(\theta,\phi)$ are radial wave function and spherical harmonics with ν, J, and m being quantum numbers associated with vibration, total angular momentum and z component of angular momentum, respectively. The radial wave functions can be obtained by solving the radial Schrödinger equation for any given total angular momentum J. For numerical implementations the final radial wave functions $\{\Psi_{\nu J}(R)\}$ and eigenenergies $\{E_{\nu J}\}$ are calculated by diagonalizing the radial Hamiltonian matrix in Fourier grid discrete variable representation.[33] The range for the numerical discretization of the internuclear distance R is [2.0, 23.0] Å with 841 equally spaced grid points.

With the help of radial wave function $\{\Psi_{\nu J}(R)\}$ and dipole moment curve, the corresponding dipole transition matrix elements $\langle \nu Jm|\mu_\gamma|\nu' J' m'\rangle$ $(\gamma = x, y, z)$ can be calculated. The photon assisted transition rates between initial state $|i\rangle$ and final state $|f\rangle$ obeys the Golden rule[34]

$$k_{fi}(\omega) = \frac{2\pi}{\hbar} \sum_{\gamma=x,y,z} |\langle f|\mu_\gamma \mathcal{E}_\gamma|i\rangle|^2 \delta(E_f - E_i - \hbar\omega) \tag{2}$$

where μ_γ and $\mathcal{E}_\gamma$ are the $\gamma = x, y, z$ components of the dipole moment and the applied external laser field, respectively. Consequently, the absorption intensity $\alpha(\omega)$ can be calculated by sum of the energy flow rate $\hbar\omega k_{fi}(\omega)$ contributed by each individual transition[34]

$$\alpha(\omega) = \frac{4\pi n\omega}{3c\varepsilon_0} \sum_{fi} \sum_{\gamma=x,y,z} P(E_i)|\langle f|\mu_\gamma|i\rangle|^2 \delta(E_f - E_i - \hbar\omega) \tag{3}$$

where n, c, and ε_0 are molecule density, light velocity, and vacuum permittivity, respectively, and $P(E_i)$ is the probability for the molecule at state $|i\rangle$. Here the intensity has been averaged over random orientations of RbCs molecules and the index i/f actually stands for three quantum numbers νJm. Applying Fourier transform to eq 3, it is not difficult to find that the absorption intensity $\alpha(\omega)$ can be calculated equivalently by Fourier transform of dipole−dipole autocorrelation function.[34] Note the delta function stands for ideal cases where each eigenstate has infinite lifetime. In reality it should be replaced by a Lorentz function to describe finite lifetime of each state.

dx.doi.org/10.1021/jp303975x | J. Phys. Chem. A 2012, 116, 11101−11106

RESULTS AND DISCUSSION

$X^1\Sigma^+$ and $a^3\Sigma^+$ Potential Energy Curves. Relativistic ab initio $X^1\Sigma^+$ and $a^3\Sigma^+$ potential curves of RbCs calculated at CCSD(T)/UGBS1P+ level with a minimum step size of 0.05 Å are shown in Figure 1. A direct scan of the potential has been performed from 2 to 23 Å for the internuclear distance R to approach the dissociation limit. However, it is always a real challenge even in present days for quantum chemistry calculations to correctly predict dissociation energies. Fortunately, the well bounded rovibrational states can still be accurately reproduced even without accurate dissociation energy up to only a global shift of energy reference, which is the main purpose of the present investigations for guidance of future experiments.

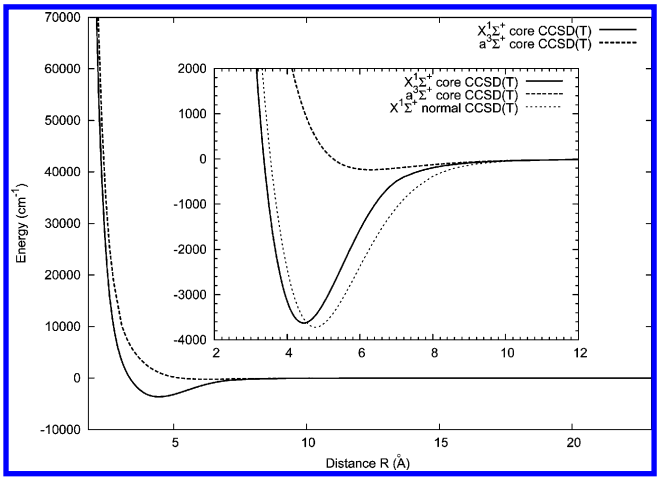

Figure 1. Relativistic ab initio $X^1\Sigma^+$ (solid) and $a^3\Sigma^+$ (dashed) potential curves of RbCs calculated at the CCSD(T)/UGBS1P+ level with an enlarged plot in the inset. Also shown in the inset is the $X^1\Sigma^+$ potential curve with one less shell of electrons for post Hartree–Fock treatment (dotted) for comparison. See the text for details.

As has already been mentioned in the Methods section, for the calculations of the potential curves one more inner shell of electrons is included for post Hartree–Fock correlation treatment than the default CCSD(T) method in Gaussian09. In the inset of Figure 1 the $X^1\Sigma^+$ potential curve calculated with default Gaussian09 CCSD(T) method has also been shown for comparison. The normal CCSD(T) method predicts the equilibrium internuclear distance, minimum of the $X^1\Sigma^+$ potential, at R = 4.75 Å (see the dotted curve). By including correlations involving one more shell of core electrons, we find the equilibrium internuclear distance to be R = 4.45 Å (the solid curves). To check the convergence of our calculations, three additional points at internuclear distances of 4.40, 4.45, and 4.50 Å have been calculated by further including one more inner shell of electrons for post Hartree–Fock correlation treatment which also finds minimum at R = 4.45 Å. Fitting the three calculated points with harmonic potential leads to minimum at R = 4.44 Å, which shows the convergence of our adopted method and the trends that including all electrons for post Hartree–Fock correlation treatment will further slightly decrease the equilibrium internuclear distance (which is, however, already reaching the limit of present supercomputers). In passing, Fellows and co-workers have derived the left and right turning points of the vibrational ground state of $X^1\Sigma^+$ state to be R = 4.315 Å and R = 4.543 Å with an average of R = 4.43 Å based on more than 23 000 observed spectral data.[35] Very recently another spectroscopy experiment has been reported for $X^1\Sigma^+$ and $a^3\Sigma^+$ states of RbCs[36] which has found the equilibrium internuclear distances of $X^1\Sigma^+$ and $a^3\Sigma^+$ states to be R = 4.427 Å and R = 6.219 Å, respectively. The equilibrium internuclear distance of our calculated $X^1\Sigma^+$ state agrees quite well with both experimentally derived results in refs 35 and 36. For $a^3\Sigma^+$ state (the dashed curves) the minimum of the potential is found to be at R = 6.30 Å which again agree well with the reported value of 6.219 Å in ref 36.

To further check the accuracy of the calculated potential curves with all-electron basis set shown in Figure 1, the vibrational eigenenergies are calculated by diagonalizing the radial Hamiltonian matrix in Fourier grid discrete variable representation. A detailed comparison between our calculated vibrational energies of the $X^1\Sigma^+$ state and previously reported ones in ref 35 is shown in Figure 2. As can be seen in Figure 2,

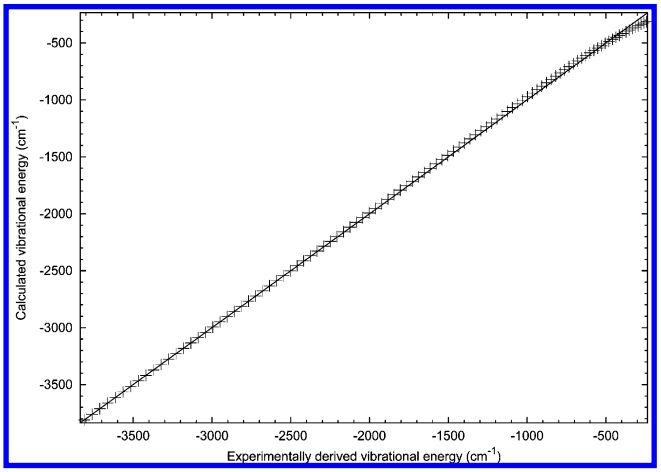

Figure 2. Comparison between calculated vibrational energy levels based on our ab initio potential and vibrational energy levels in ref 35 based on observed spectral data of $X^1\Sigma^+$ state (scattered points). The reference that indicates exact agreement (solid straight line) is also shown.

the vibrational energies of the $X^1\Sigma^+$ state calculated from our ab initio potential agree well with the ones reported in ref 35, which are based on experimental spectral data. Large deviations are only found for levels near the dissociation limit due to the lower accuracy of our potential at dissociation distance, which is generally considered a major difficulty of ab initio calculations. The calculated dissociation energies for $X^1\Sigma^+$ and $a^3\Sigma^+$ states are 3629 and 238 cm^{-1}, respectively, which are underestimated compared to the very recently reported experimental dissociation energies of 3836.37 cm^{-1} for $X^1\Sigma^+$ and 259.34 cm^{-1} for $a^3\Sigma^+$ in ref 36. In principle, the accuracy of the dissociation energy can be improved by more accurate methods and larger basis sets when even powerful computers are available in the future. Or an even better way may be to fit accurate parameters for the analytic potential energy function according to the induced dipole–dipole interactions of Rb and Cs atoms at large distance. However, less accuracy of the potential curve at the dissociation limit does not affect the accuracy of our most interested topics in the present work because we do not focus on energies of the vibrational levels near dissociation limit. For the convenience of future investigations all the calculated rovibrational energy levels are reported with respect to the experimental RbCs dissociation

dx.doi.org/10.1021/jp303975x | J. Phys. Chem. A 2012, 116, 11101–11106

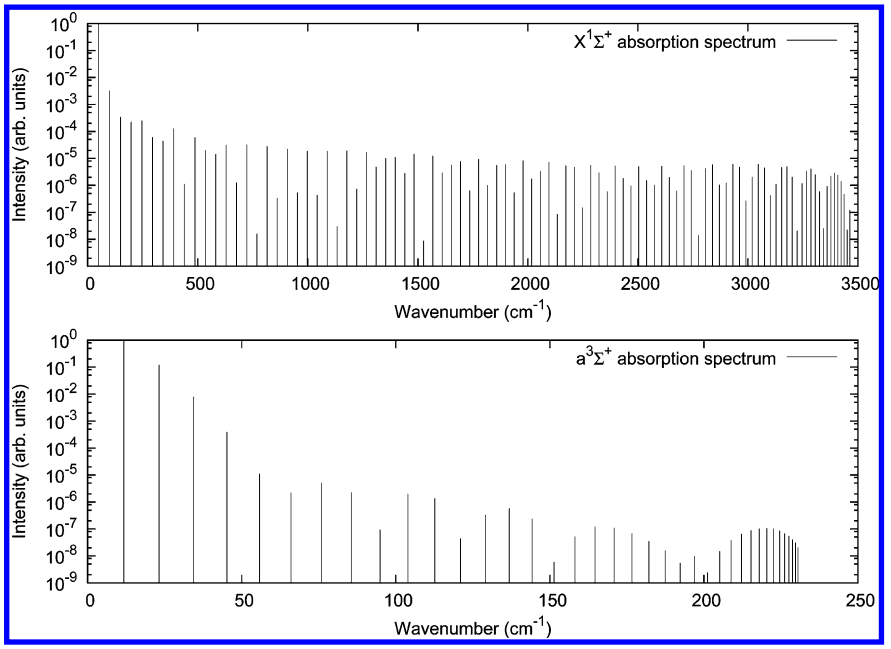

Figure 3. Vibrational absorption spectra of cold/ultracold RbCs molecules for arbitrary temperature lower than 1 K in logarithm scale. Top: $X^1\Sigma^+$ state. Bottom: $a^3\Sigma^+$ state. Intensities are normalized with respect to the most intense transitions.

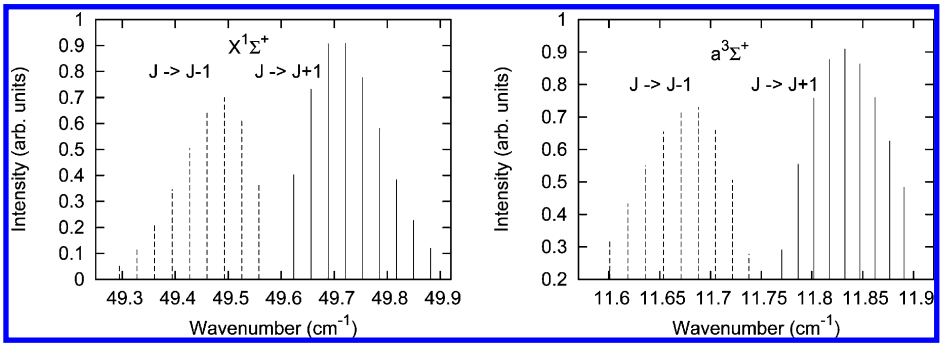

Figure 4. Rotationally resolved absorption spectra of cold/ultracold RbCs molecules. Intensities are normalized with respect to the most intense transitions. Left: $X^1\Sigma^+$ state RbCs at 0.5 K. Right: $a^3\Sigma^+$ state RbCs at 0.5 K.

limit according to the accurate experimental dissociation energies of lowest $^{1,3}\Sigma^+$ states in ref 36. With respect to this energy reference the calculated rovibrational ground state energies of $X^1\Sigma^+$ and $a^3\Sigma^+$ states are −3811.0 and −253.2 cm^{-1}, respectively. More information about the vibrational energy levels of lowest $^{1,3}\Sigma^+$ states not so close to the corresponding dissociation limit are available in the Supporting Information.

Rovibrational Spectra of RbCs at Lowest $^{1,3}\Sigma^+$ States. Figure 3 shows the vibrational absorption spectra of cold/ultracold RbCs molecules at its lowest $^{1,3}\Sigma^+$ states. For arbitrary temperature lower than 1 K, the vibrational absorption spectra are almost the same as shown in Figure 3. The most intense absorption band is contributed by $|0Jm\rangle$ to $|1J'm'\rangle$ ($J' = J \pm 1$) series of excitations for both $X^1\Sigma^+$ (top panel) and $a^3\Sigma^+$ (bottom panel) states. It has an intensity much stronger than other bands by at least 2 orders of magnitude for the $X^1\Sigma^+$ state and 1 order of magnitude for the $a^3\Sigma^+$ state. Exponential decay of the absorption intensity is found for the first few absorption bands when laser frequency is increased due to decay of overlap between $|0Jm\rangle$ and $|\nu J'm'\rangle$. For much higher vibrational excitations, there exist some local maxima of absorption intensity that might be interesting for transferring highly excited vibrational states to the ground state. Compared with the $X^1\Sigma^+$ state, the $a^3\Sigma^+$ state potential curve is more flat; therefore, the vibrational ground state wave function is more delocalized, leading to the fact that the overlap with other states decay more slowly.

To gain more insight into the $|0Jm\rangle$ to $|1J'm'\rangle$ series of transitions, the rotationally resolved absorption spectra of cold/ultracold RbCs molecules at lowest $^{1,3}\Sigma^+$ states are shown in Figure 4. The intensities reported in Figure 4 are $|0J\rangle$ to $|1J'\rangle$ transitions with analytical average/sum over all possible m/m' according to eq 3. The $|0J\rangle$ to $|1,J+1\rangle$ ($J = 0, 1, 2, ...$) transitions are shown in solid lines and the $|0J\rangle$ to $|1,J-1\rangle$ ($J = 1, 2, ...$) transitions in dashed lines. The left panel shows the absorption spectrum of RbCs at the $X^1\Sigma^+$ state with a temperature of 0.5 K when many rotational states can be populated at thermal equilibrium. When the temperature decreases to lower than 1 mK, only $|000\rangle$ can be significantly populated for both two $^{1,3}\Sigma^+$ states according to the rotational excitation energies. The $|000\rangle$ to $|100\rangle$ (forbidden transition) excitation energy is 49.6 cm^{-1} for the $X^1\Sigma^+$ state, which agrees well with the reported value of 49.8 cm^{-1} in ref 35 and also agrees with previous experiment.[6] For the $a^3\Sigma^+$ state our calculated $|000\rangle$ to $|100\rangle$ excitation energy is 11.8 cm^{-1} . The rotational constants can be fitted to be 0.0163 cm^{-1} for $X^1\Sigma^+$ state and 0.0081 cm^{-1} for $a^3\Sigma^+$ state.

dx.doi.org/10.1021/jp303975x | J. Phys. Chem. A 2012, 116, 11101−11106

Finally, as has been mentioned in the Methods section, the spin−orbit effects are not calculated because they have been reported to be ignorable for the lowest $^{1,3}\Sigma^+$ states. For Σ states the electronic total orbital angular momentum is zero along the internuclear axis, consequently the spin−orbit coupling is ignorable, which can be best described by Hund's case (b). The ignorable spin−orbit effects are the major reason for the metastable characteristics of the $a^3\Sigma^+$ state. For Hund's case (b) the rotation of the molecule will couple to the triplet electronic spin states. Similar to the standard term for spin−orbit coupling, the coupling between the molecule rotation and electron spin is proportional to q^2/μ^2R^3. Compared to a single electron spin−orbit coupling, the RbCs partial charge q is about 1/10 of electron charge, the reduced mass μ is about 10^5 times of electron mass and the internuclear distance R is about 10 times of Bohr radius. Therefore, the fine structure couplings can be ignored for the investigated rovibrational levels of the lowest $^{1,3}\Sigma^+$ states.

To summarize the investigated lowest $^{1,3}\Sigma^+$ states, a detailed comparison between the present work and previous experimental and theoretical work is provided in Table 1 for potentials and molecular properties including equilibrium internuclear distance R_e, dissociation energy D_e, $|000\rangle$ to $|100\rangle$ transition frequency ω_{10}, and rotational constants B_e. Results of the present work agree quite well with experimental data except for the dissociation energy. Additional analysis based on observed transition frequencies reported in ref 36 are also provided for comparison. For the $X^1\Sigma^+$ state the observed energy difference between $|0, 301, m\rangle$ and $|1, 301, m\rangle$ is 46.084 cm^{-1}. Assuming $E_{vJm} = E_{v00} + J(J+1)B_e$ and using the reported $B_e(v=0) - B_e(v=1) = 4.1 \times 10^{-5}$ cm^{-1}, the transition frequency ω_{10} for the $X^1\Sigma^+$ state is 49.81 cm^{-1}. Similarly, ω_{10} for the $a^3\Sigma^+$ state is derived to be 11.71 cm^{-1} based on the observed energy difference of 11.687 cm^{-1} between $|0, 71, m\rangle$ and $|1, 71, m\rangle$ states. The rotational constants are also derived to be 15.3×10^{-3} and 8.2×10^{-3} cm^{-1}, respectively for the $X^1\Sigma^+$ and $a^3\Sigma^+$ states with the observed energy differences between $|0, J, m\rangle$ and $|0, J', m'\rangle$. Note these two numbers provide lower limits for corresponding rotational constants because B_e slightly decreases with quantum number J. The derived rotational constant $B_e = 15.3 \times 10^{-3}$ cm^{-1} is for $J = 301$ and $B_e = 8.2 \times 10^{-3}$ cm^{-1} is for $J = 71$ (both are the lowest observed ones). The convergence of the present study is verified by increasing the level of the adopted method for the $X^1\Sigma^+$ state. Clear trends of increasing of accuracy are found for increasing the level of calculations step by step, which shows the advantage of using all-electron basis sets. Based on the convergence verification, an estimation of uncertainties of the major reported results in the present work will be briefly discussed. For the equilibrium internuclear distances the reported values provide upper limits according to our three different levels of calculations for the $X^1\Sigma^+$ state. According to the trends of improvements the error of $R_e = 4.44$ Å for the $X^1\Sigma^+$ state is about [−0.02, 0] Å, whereas for $a^3\Sigma^+$ no further accurate calculations are made and the error for $R_e = 6.30$ Å is about [−0.1, 0.05] Å. Concerning the vibrational energies, the diagonalization of the radial Hamiltonian in Fourier grid discrete variable representation has an error of less than 0.1%; consequently, major errors are caused by potentials. By comparison of various levels of calculations for the $X^1\Sigma^+$ state, this error is estimated to be less than 1% for ω_{10}. For the two lowest $^{1,3}\Sigma^+$ states the estimated errors for ω_{10} and B_e are about [−0.4, 0.4] and [−0.4, 0.4] $\times 10^{-3}$ cm^{-1}, respectively. To be safe, all the reported uncertainties for the calculated results are upper limits, which means real errors are smaller than the estimated ones.

Table 1. Comparison between Present and Existing Theoretical and Experimental Work on RbCs Lowest $^{1,3}\Sigma^+$ States[a]

$X^1\Sigma^+$	R_e (Å)	D_e (cm^{-1})	ω_{10} (cm^{-1})	B_e (10^{-3} cm^{-1})
this work CC1[b]	4.45(10)	3629	49.6(4)	16.3(4)
this work CC2[c]	4.44(2)	3643		
experiment[d]	4.43*	3836.1(5)	49.8	16.6
experiment[e]	4.427	3836.37(4)	49.8*	15.3*[LL]
theory[f]	4.38, 4.38	3873, −	51.4, 51.3	16.9, 16.9
theory[g]	4.36, 4.47	4033, −	49.1, 52	16.89, −
$a^3\Sigma^+$	R_e (Å)	D_e (cm^{-1})	ω_{10} (cm^{-1})	B_e (10^{-3} cm^{-1})
this work CC1[b]	6.30(10)	238	11.8(4)	8.1(4)
experiment[e]	6.22	259.34(3)	11.7*	8.2*[LL]
theory[f]	5.84, 6.18	−, −	42.8, 12.6	9.5, 8.5
theory[g]	6.57, 6.30	116, 245	−, 12	−, −

[a]The equilibrium internuclear distance R_e, dissociation energy D_e, $|000\rangle$ to $|100\rangle$ transition frequency ω_{10}, and rotational constants B_e are compared with available uncertainties shown in brackets. Experimental results without explicitly written uncertainties are accurate for the given digits. [b]Including one more inner shell of electrons than Gaussian 09 default for correlation. [c]Including two more inner shell of electrons than Gaussian 09 default for correlation, only calculate three points around 4.45 Å and one point at 23 Å. [d]Reference 35. The number labeled by star is derived from reported turning points. [e]Reference 36. Numbers labeled by stars are derived from observed transition frequencies. For rotational constants only lower limits are provided. [f]References 23 and 24. [g]Results from ref 25 using two different pseudopotentials by Lim and co-workers.

CONCLUSIONS

In conclusion, the present work shows the accuracy of the calculated potential energy curves of RbCs at the lowest $^{1,3}\Sigma^+$ states with all-electron basis set and absorption spectra based on these potentials. The calculated potential curves are accurate except at large internuclear distances where standard quantum chemistry programs encounter their bottleneck. However, the potential function at large internuclear distances can be fitted by experimental data or extremely high level calculations when necessary. The equilibrium internuclear distances are found to be at $R = 4.44$ Å for the $X^1\Sigma^+$ state and at $R = 6.30$ Å for the $a^3\Sigma^+$ state, which agree with previous experiments. The calculated lowest $^{1,3}\Sigma^+$ potential curves with an all-electron basis set are expected to be a good basis for further investigations on RbCs molecules. It should be noted that it is straightforward to increase the accuracy of potential curves calculated with an all-electron basis set in the future when necessary.

For investigations not involving rovibrational states near the dissociation limit the present potentials already give accurate results. Our calculated rovibrational energy levels agree well with previous experimental and theoretical work. The calculated fundamental excitation frequency for RbCs vibration is 49.6 cm^{-1} at the $X^1\Sigma^+$ state and 11.8 cm^{-1} at the $a^3\Sigma^+$ state. Rotational constants for the two states are 0.0163 and 0.0081 cm^{-1}, respectively. The study of absorption spectra provide a reference for further experiments of RbCs manipulations in the future especially when the ground state RbCs ensemble is obtained. When more potential curves with sufficient accuracy

are available, it should be quite promising to theoretically design accurate pathways to produce dense ensemble of RbCs molecules at both electronic and rovibrational ground state and further manipulation schemes.

■ ASSOCIATED CONTENT

Supporting Information

Table 1: vibrational energy levels of $X^1\Sigma^+$ and $a^3\Sigma^+$ states with respect to the dissociation limit. Levels close to the dissociation limit are not reported due to less accuracy of the present treatment for them. Convergence test of vibrational energy levels of $X^1\Sigma^+$ states are also available. Various calculations are made using the grid region of $[R_{min}, R_{max}]$ to report the lowest N vibrational energy levels. In all the calculations R_{min} = 2.0 Å is fixed while R_{max} and N are adjusted to test the convergence. Table 2: root-mean-square deviations of calculated vibrational energy levels between small R_{max} and the converged one R_{max} = 50.0 Å. This material is available free of charge via Internet at http://pubs.acs.org.

■ AUTHOR INFORMATION

Corresponding Author

*E-mail: ygyang@sxu.edu.cn.

Notes

The authors declare no competing financial interest.

■ ACKNOWLEDGMENTS

This work was supported in part by 973 Program of China under Grant No. 2012CB921603, the National Natural Science Foundation of China under Grant No. 11004125, International Science & Technology Cooperation program of China (2011DFA12490), National Natural Science Foundation of China under Grant Nos. 10934004 and 60978018, and NSFC Project for Excellent Research Team (61121064).

■ REFERENCES

(1) Santos, L.; Shlyapnikov, G. V.; Zoller, P.; Lewenstein, M. *Phys. Rev. Lett.* **2000**, *85*, 1791.

(2) DeMille, D. *Phys. Rev. Lett.* **2002**, *88*, 067901.

(3) Carr, L. D.; DeMille, D.; Krems, R. V.; Ye, J. *New J. Phys.* **2009**, *11*, 055049.

(4) Dulieu, O.; Gabbanini, C. *Rep. Prog. Phys.* **2009**, *72*, 086401.

(5) Ospelkaus, S.; Ni, K.-K.; Wang, D.; de Miranda, M. H. G.; Neyenhuis, B.; Quéméner, G.; Julienne, P. S.; Bohn, J. L.; Jin, D. S.; Ye, J. *Science* **2010**, *327*, 853.

(6) Sage, J. M.; Sainis, S.; Bergeman, T.; DeMille, D. *Phys. Rev. Lett.* **2005**, *94*, 203001.

(7) Deiglmayr, J.; Grochola, A.; Repp, M.; Mörtlbauer, K.; Glück, C.; Lange, J.; Dulieu, O.; Wester, R.; Weidemüller, M. *Phys. Rev. Lett.* **2008**, *101*, 133004.

(8) Ni, K.-K.; Ospelkaus, S.; de Miranda, M. H. G.; Péer, A.; Neyenhuis, B.; Zirbel, J. J.; Kotochigova, S.; Julienne, P. S.; Jin, D. S.; Ye, J. *Science* **2008**, *322*, 231.

(9) Ospelkaus, S.; Péer, A.; Ni, K.-K.; Zirbel, J. J.; Neyenhuis, B.; Kotochigova, S.; Julienne, P. S.; Ye, J.; Jin, D. S. *Nat. Phys.* **2008**, *4*, 622.

(10) Aikawa, K.; Akamatsu, D.; Hayashi, M.; Oasa, K.; Kobayashi, J.; Naidon, P.; Kishimoto, T.; Ueda, M.; Inouye, S. *Phys. Rev. Lett.* **2010**, *105*, 203001.

(11) Wang, D.; Qi, J.; Stone, M. F.; Nikolayeva, O.; Wang, H.; Hattaway, B.; Gensemer, S. D.; Gould, P. L.; Eyler, E. E.; Stwalley, W. C. *Phys. Rev. Lett.* **2004**, *93*, 243005.

(12) Ridinger, A.; Chaudhuri, S.; Salez, T.; Fernandes, D. R.; Bouloufa, N.; Dulieu, O.; Salomon, C.; Chevy, F. *Eur. Phys. Lett.* **2011**, *96*, 33001.

(13) Stan, C. A.; Zwierlein, M. W.; Schunck, C. H.; Raupach, S. M. F.; Ketterle, W. *Phys. Rev. Lett.* **2004**, *93*, 143001.

(14) Hodby, E.; Thompson, S. T.; Regal, C. A.; Greiner, M.; Wilson, A. C.; Jin, D. S.; Cornell, E. A.; Wieman, C. E. *Phys. Rev. Lett.* **2005**, *94*, 120402.

(15) Wille, E.; Spiegelhalder, F. M.; Kerner, G.; Naik, D.; Trenkwalder, A.; Hendl, G.; Schreck, F.; Grimm, R.; Tiecke, T. G.; Walraven, J. T. M.; Kokkelmans, S. J. J. M. F.; Tiesinga, E.; Julienne, P. S. *Phys. Rev. Lett.* **2008**, *100*, 053201.

(16) Pilch, K.; Lange, A. D.; Prantner, A.; Kerner, G.; Ferlaino, F.; Nägerl, H.-C.; Grimm, R. *Phys. Rev. A* **2009**, *79*, 042718.

(17) Żuchowski, P. S.; Hutson, J. M. *Phys. Rev. A* **2010**, *81*, 060703.

(18) Kerman, A. J.; Sage, J. M.; Sainis, S.; Bergeman, T.; DeMille, D. *Phys. Rev. Lett.* **2004**, *92*, 033004.

(19) Kerman, A. J.; Sage, J. M.; Sainis, S.; Bergeman, T.; DeMille, D. *Phys. Rev. Lett.* **2004**, *92*, 153001.

(20) Gabbanini, C.; Dulieu, O. *Phys. Chem. Chem. Phys.* **2011**, *13*, 18905−18909.

(21) Ji, Z.; Zhang, H.; Wu, J.; Yuan, J.; Yang, Y.; Zhao, Y.; Ma, J.; Wang, L.; Xiao, L.; Jia, S. *Phys. Rev. A* **2012**, *85*, 013401.

(22) Debatin, M.; Takekoshi, T.; Rameshan, R.; Reichsöllner, L.; Ferlaino, F.; Grimm, R.; Vexiau, R.; Bouloufa, N.; Dulieu, O.; Nägerl, H.-C. *Phys. Chem. Chem. Phys.* **2011**, *13*, 18926−18935.

(23) Allouche, A. R.; Korek, M.; Fakherddin, K.; Chaalan, A.; Dagher, M.; Taher, F.; Aubert-Frcon, M. *J. Phys. B* **2000**, *33*, 2307.

(24) Fahs, H.; Allouche, A. R.; Korek, M.; Aubert-Frécon, M. *J. Phys. B* **2002**, *35*, 1501.

(25) Lim, I. S.; Lee, W. C.; Lee, Y. S.; Jeung, G.-H. *J. Chem. Phys.* **2006**, *124*, 234307.

(26) Aymar, M.; Dulieu, O. *J. Chem. Phys.* **2005**, *122*, 204302.

(27) Kotochigova, S.; Tiesinga, E. *J. Chem. Phys.* **2005**, *123*, 174304.

(28) Deiglmayr, J.; Aymar, M.; Wester, R.; Weidemüller, M.; Dulieu, O. *J. Chem. Phys.* **2008**, *129*, 064309.

(29) Azizi, S.; Aymar, M.; Dulieu, O. *Eur. Phys. J. D* **2004**, *31*, 195−203.

(30) Londoño, B. E.; Mahecha, J.; Luc-Koenig, E.; Crubellier, A. *Phys. Chem. Chem. Phys.* **2011**, *13*, 18738−18754.

(31) Frisch, M. J. et al. *Gaussian 09*, Revision B.01; Gaussian Inc.: Wallingford, CT, 2010.

(32) deJong, W. A.; Harrison, R. J.; Dixon, D. A. *J. Chem. Phys.* **2001**, *114*, 48−53.

(33) Marston, C. C.; Balint-Kurti, G. G. *J. Chem. Phys.* **1989**, *91*, 3571−3577.

(34) May, V.; Kühn, O. *Charge and Energy Transfer Dynamics in Molecular Systems*, 3rd revised and enlarged ed.; Wiley-VCH: Weinheim, 2011.

(35) Fellows, C. E.; Gutterres, R. F.; Campos, A. P. C.; Vergès, J.; Amiot, C. *J. Mol. Spectrosc.* **1999**, *197*, 19.

(36) Docenko, O.; Tamanis, M.; Ferber, R.; Knöckel, H.; Tiemann, E. *Phys. Rev. A* **2011**, *83*, 052519.